Effect of Geometrical Discontinuity on Ductile Fracture Initiation Behavior under Static Loading

G. -B. An, M. Ohata and M. Toyoda

Abstract

It is important to evaluate the fracture initiation behaviors of steel structure. It has been well known that the ductile cracking of steel would be accelerated by triaxial stress state. Recently, the characteristics of critical crack initiation of steels are quantitatively estimated using the two-parameters, that is, equivalent plastic strain and stress triaxiality, criterion.

This study is paid to the fundamental clarification of the effect of notch radius, which can elevate plastic constraint due to heterogeneous plastic straining on critical condition to initiate ductile crack using two-parameters. Hense, the crack initiation testing were conducted under static loading using round bar specimens with circumferential notch. To evaluate the stress/strain state in the specimens was used thermal elastic-plastic FE-analysis.

The result showed that equivalent plastic strain to initiate ductile crack expressed as a function of stress triaxiality obtained from the homogeneous specimens with circumferential notched under static loading. And it was evaluated that by using this two-parameters criterion, the critical crack initiation of homogeneous specimens under static loading.

Key Words : Ductile crack initiation, Static loading, Stress triaxiality, Equivalent plastic strain.

1. Introduction

Brittle failure of high toughness steel structures tends to occur after ductile crack initiation/propagation. The damage of steel structures in the Hanshin Great Earthquake has been reported in references [1-3]. Several brittle failures were observed in the beam-to-column connection zones where there exists geometrical discontinuity. In some of them, brittle fracture occurred after large scale plastic deformation associated with ductile crack initiation and extension from stress/strain concentrators.

It is important to estimate ductile crack initiation and propagation followed by brittle fracture. On the basis of ductile crack initiation behavior, the ductile cracking controlling mechanical parameters were expressed in terms of two parameters, that is equivalent plastic strain $\bar{\varepsilon}_p$, and stress triaxiality $\sigma_m/\bar{\sigma}$, based on void growth mechanism[4]. It has been shown by experiments using circumferentially notched specimens that the critical strain for ductile fracture initiation was decreased with increasing stress triaxiality associated with notch acuity[5-10]. A quantitative evaluation of ductile fracture initiation has been developed using the two-parameter criterion[7-10].

The present study focuses on the fundamental clarification of the effects of geometrical heterogeneity on the critical condition to initiate ductile fracture. The main attention was paid to the applicability of the two-parameter criterion to the estimation of ductile cracking for homogeneous specimens under static tensile loading condition. Ductile crack initiation testing was conducted under static loading using circumferentially notched round bar specimens with / without. Moreover, in order to evaluate the stress/strain behavior in the specimen under static loading with high accuracy, thermal elastic—plastic FE-analyses were carried out. It is shown that the condition for ductile crack initiation using the two parameters, that is equivalent plastic strain and stress triaxiality.

2. Experimental methods

Round bar tensile specimens with diameter of 10 mm were used. In the homogeneous specimens two types of circumferential notch shown in Fig. 1 were employed to

G. -B. An, M. Ohata and *M. Toyoda* : Department of Manufacturing Science, Osaka University, Osaka, Japan
E-mail : angb@mech.eng.himeji-tech.ac.jp

Table 1 Chemical composition of *HT*50 steel used.

Steel	C	Si	Mn	P	S	Cu	Ni	Cr	Mo	V	Ti	Nb	Al	B	C_{eq}	P_{cm}
HT50	0.17	.031	1.48	0.011	0.002	-	-	-	-	-	-	-	0.016	-	0.43	0.25

$C_{eq} = C + Mn/6 + (Cr + Mo + V)/5 + (Cu + Ni)/15$

$P_{cm} = C + si/30 + Mn/20 + Cu/20 + Ni/60 + Cr/20 + Mo/15 + V/10 + 5B$

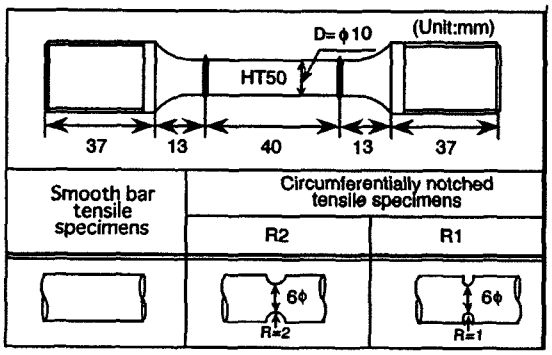

Fig. 1 Configuration of round-bar tensile specimens with geometrical heterogeneity

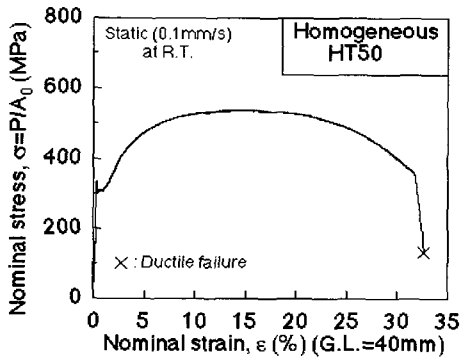

Fig. 2 Nominal stress σ — nominal strain ε curve for homogeneous specimen under static loading, 0.1 mm/s

quantify the effect of stress triaxiality on ductile cracking behavior. These specimens were extracted from *HT*50 plate.

Table 1 shows the chemical composition of the *HT*50 steel used. The nominal stress—nominal strain curve for *HT*50 steel is shown in Fig. 2. The mechanical properties of the *HT*50 steel is summarized in Table 2.

Tensile test were carried out at cross head displacement speeds at 0.1 mm/s (static loading) at room temperature. The experimental equipment was a servo—hydraulic high loading rate tension test machine.

Table 2 Mechanical properties of steel used

Steel	σ_Y (MPa)	σ_T (MPa)	YR (%)	ε_T (%)	EL (%)	RA (%)
HT50	298	522	57	14.1	30.8	68

σ_Y : Lower yield stress
σ_T : Tensile strength
YR : Yield-to-tensile ratio (σ_Y / σ_T)
ε_T : Uniform elongation
EL : Elongation (G. L. = 40mm, Dia. = 10mm)
RA : Reduction in area
$S_r(Y)$: ${\sigma_Y}^{HT80} / {\sigma_Y}^{HT50}$
$S_r(T)$: ${\sigma_T}^{HT80} / {\sigma_T}^{HT50}$

3. Ductile crack initiation behavior of homogeneous specimens under static loading

The ductile crack initiation behavior of a homogeneous (*HT*50 steel) round bar specimen with/without circumferential notch under static loading is shown in Fig. 3.

An inflection point in the load—displacement curve appeared just before final ductile failure in all specimens. Just after the inflection point, the specimens fractured accompanied by rapid load-decrease. The specimens after fracture exhibited typical cup and cone type fracture, and equiaxed dimples were observed in the central region of the fracture surface.

Ductile crack initiation behavior was observed using scanning electron microscope (SEM) at longitudinal cross-section in the vicinity of center of specimens which were unloaded just before and after the inflection point. Fig. 4 shows an example for *R*2—type specimen which

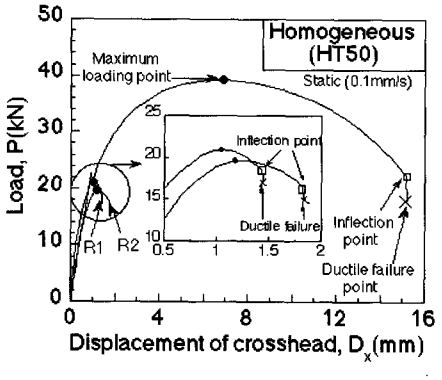

Fig. 3 Load P—cross head displacement D_X curves obtained by tensile tests for smooth and circumferentially notched specimens under static loading, 0.1 mm/s

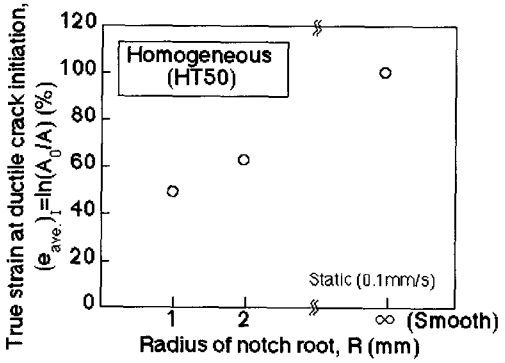

Fig. 5 Effect of notch radius R, on ductile crack initiation strain $(e_{ave.})_I$, in homogeneous $HT50$ specimens

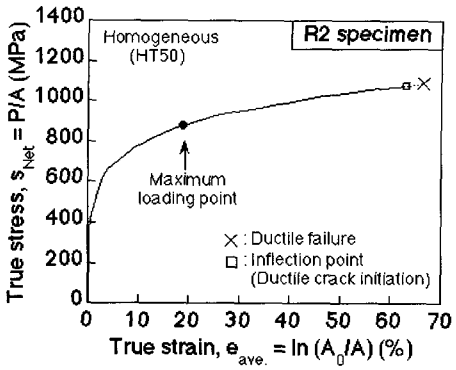

(a) True stress—True strain curve

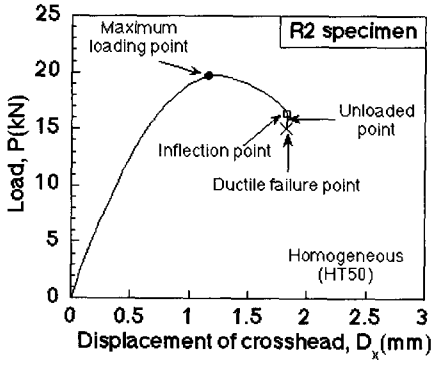

(b) P — D_X curve

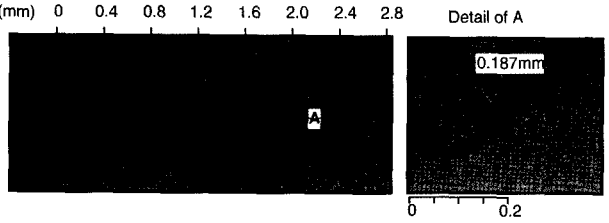

(c) SEM micrographs of the specimen sectioned near the center of specimen just before ductile failure

Fig. 4 Ductile crack initiation behavior of $R2$ specimen under static loading, 0.1 mm/s

was unloaded just after the inflection point as shown in the figure. The microscopic observations show that ductile cracking occurs associated with growth and coalescence of large number of micro-voids generated between large scale voids in the vicinity of the center of the necking region. Similar results were also observed in smooth and $R1$—type specimens. According to this observation, the rapid load reduction just before final ductile failure is supposed to result in ductile cracking in the central region of the specimen, and subsequent rapid ductile crack propagation to the specimen surface leads to final failure. Consequently, in the present study, ductile crack initiation was defined to occur at the inflection point observed in the load P versus cross head displacement D_X curves.

Fig. 5 shows the critical strain $(e_{ave.})_I$ (= average true strain in the net section) at ductile crack initiation obtained from specimens with various circumferential notches. The critical strain for ductile crack initiation is affected by stress triaxiality, and the critical strain becomes smaller with decreasing radius of notch root.

4. Applicability of two-parameter ductile cracking criterion to homogeneous specimens under static loading in single tension

The dependence of triaxial stress state on ductile crack initiation in materials has been widely expressed by using two parameters, equivalent plastic strain and stress triaxiality[4-10]. This is because of that the ductile cracking from inter-specimen under single tensile loading is generally controlled by voids behaviors of which growth is theoretically derived to be enlarged by high stress triaxiality[4]. The authors have been paid attention to the transferability of local mechanical condition for ductile cracking using two parameters obtained by homogeneous specimens with/without notch subjected to single tension to ductile cracking estimation for the other specimens which give different triaxial stress state[9].

4.1 Numerical analysis

In order to estimate the mechanical condition to initiate ductile crack, stress and strain state in the local area of specimens in which ductile cracking occurred should be precisely estimated, because stress / strain distribution in the minimum cross section would not be constant in homogeneous tensile specimen. The FEM was used for analyzing the stress/strain state in the specimen.

The FE—analysis taking into account heat generation and conduction was carried out using the finite element code ABAQUS version 5.8[11]. In this coupled thermal elastic-plastic FE—analysis, 90% of the plastic work generated was assumed to be converted into heat followed by temperature rise[12-14]. The physical properties shown in Table 3 were used for heat conduction and thermal-stress analysis.

The all specimens used in the experiments were modeled with axi-symmetrical four-node isoparametric elements. Fig. 6 shows the examples of mesh division for smooth homogeneous specimen and notched specimen (*R*2). The minimum mesh size is 0.03 mm×0.03 mm at the cross-section in the middle of all specimens. Large deformation considering nonlinear geometric properties are adopted in this analysis.

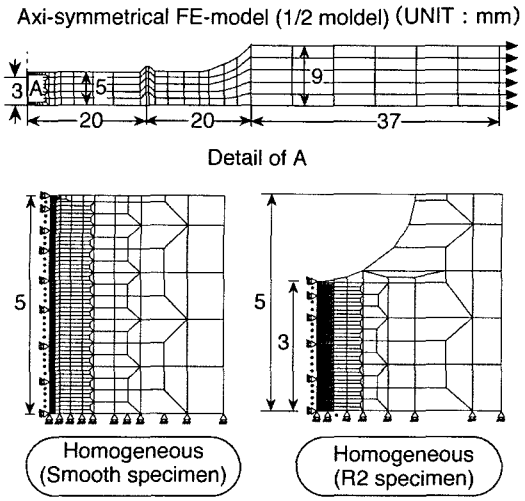

Fig. 6 Mesh division of models used for FE—analysis

The results of FE-analysis are compared with experimental data in Fig. 7, for smooth homogenous specimen under static loading (0.1 mm/s). The analyzed global deformation behavior, that is nominal stress—nominal strain relation to failure give good agreement with the experimental results. Consequently, FE—analytical method employed in this study can accurately provide local stress—strain state in the specimen under static loading.

Table 3 Material constant used for coupled thermal elastic – plastic FE-analysis

Steel	E (Gpa)	ν	c (J/kg·K)	ρ (kg/mm^3)	κ (m^2 /s)	β (1/K)
HT50	206	0.3	4.8×10^2	8.0×10^{-6}	2.17×10^{-5}	1.2×10^{-5}

E : Young's modulus
c : Specific heat
κ : Heat conductivity
ν : Poisson's ratio
ρ : Density
β : Cofficient of heat

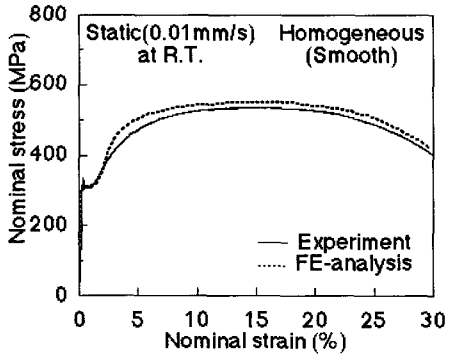

Fig. 7 Comparison of experimental and numerical nominal stress σ — nominal strain ε curves in homogeneous specimen under static loading, 1mm/s

4.2 Critical condition for ductile crack initiation in specimens with geometrical discontinuity under static loading

The critical condition for ductile crack was examined using FE—analysis of homogeneous round-bar specimens (*HT*50 steel) with/without circumferential notch under static loading (0.1 mm/s). Fig. 8 shows the distribution of equivalent plastic strain $\bar{\varepsilon}_p$ and stress triaxiality $\sigma_m / \bar{\sigma}$ (σ_m : mean stress, $\bar{\sigma}$: Von Mises equivalent stress) along the net section of *R*2 specimen at the critical stain level ($(e_{ave.})_I$ = 60%) for ductile crack initiation. The stress triaxiality is maximal in the center of the specimen, on the contrary equivalent plastic strain is the largest in the surface of the notch root. However, both the equivalent plastic strain and the stress triaxiality are almost constant in the vicinity of the specimen center where ductile crack nucleated.

The critical conditions for ductile cracking should be estimated by using local mechanical parameters at which ductile cracking occurred in experiments. Using FE—analytical results and comparing experimental results, the relationship between equivalent plastic strain $\bar{\varepsilon}_p$ and stress triaxiality $\sigma_m / \bar{\sigma}$ in the center of specimen when ductile crack initiated was plotted for smooth, *R*2 and *R*1 type specimens. As shown in Fig. 9, the local critical equivalent plastic strain $(\bar{\varepsilon}_p)_{cr}$ is decreased with increasing of the stress triaxiality $\sigma_m / \bar{\sigma}$ accompanied by notch acuity. This local condition for ductile cracking using two parameters, that is critical equivalent plastic strain as a function of the stress triaxiality just fitted by equation (1), would be expected to be a criterion for ductile crack initiation.

$$\bar{\varepsilon}_p = a + b \cdot \exp(-c \ \sigma_m / \bar{\sigma}) \quad (1)$$

where, a (= 0.1), b (= 4.82) and c (= 1.92) are constants.

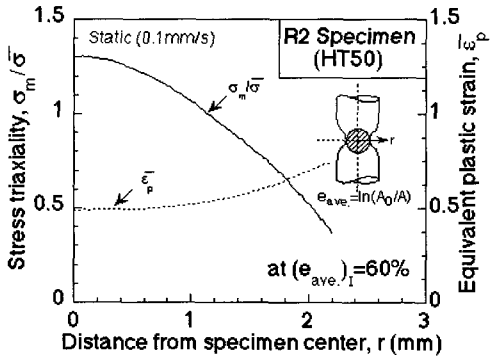

Fig. 8 Distribution of equivalent plastic strainand stress triaxiality in the minimum cross-section of specimen at under static loading, .

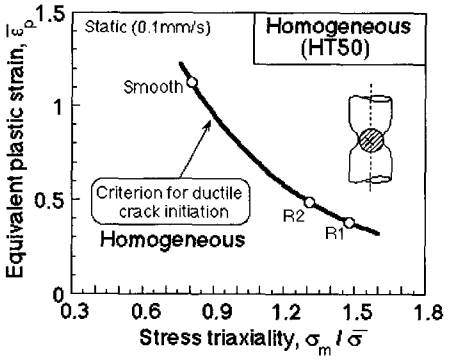

Fig.9 Condition for ductile cracking using two parameters equivalent plastic strainand stress triaxiality, for steel under static loading, .

5. Conclusion

This study was mainly paid attention to the transferability of local mechanical condition for ductile cracking using two parameters, that is equivalent plastic strain $\bar{\varepsilon}_p$ and stress triaxiality $\sigma_m / \bar{\sigma}$, obtained by homogeneous specimens with / without notch subjected

to single tension to ductile cracking estimation under static loading. Tensile tests under static loading was conducted on round bar specimens which have different plastic constraint by circumferential notch. In order to address the local stress-strain state in the specimens for estimating local ductile crack criterion, numerical calculations based on coupled thermal elastic-plastic FE—analyses were carried out. It was substantiated that local critical condition for ductile crack initation for homogenous specimens under static loading were estimated using two parmeter based on equivalent plastic strain and stress triaxiality.

References

1. AIJ : Reconnaissance report on damage of steel building structures observed from the 1995 hyogoken-nanbu(hanshin/awaji) earthquake, *Steel Committee of Kinki Branch*, (1995)
2. M. Toyoda : How steel structures fared in japan great earthquake, *Welding Journal*, Vol. 74, No. 12 (1995), pp. 132s-136s
3. K. Okashita , R. Ohminami, K. Michiba, A. Yamamoto, M. Tomimatsu, Y. Tanji and C. Miki : Investigation of the brittle fracture at the corner of p75 rigid-frame pier in kobe harbor highway during the hyogoken-nanbu earthquake, *Journals of the Japan Society of Civil Engineers*, Vol. 591, No. I-43 (1998), pp. 243-261
4. F. A. McClintock : A criterion for ductile fracture by the growth of holes, *Journal of Applied Mechanics Transactions of the ASME*, Vol. 35, (1968), pp. 363-371
5. A. C. Mackenzie, J. W. Hancock and K. K. Brown : On the influence of state of stress on ductile failure initiation in high strength steels, *Engineering Fracture Mechanics*, Vol. 9, (1977), pp. 167-188
6. J. W. Hancock and A. C .Mackenzie : On the mechanisms of ductile failure in high-strength steels subjected to multi-axial stress-states, *Journal of Mech. Phys. Solids*, Vol. 24, (1976), pp. 147-169
7. A. Otsuka, T. Miyata, S. Nishimura, M. Kimura and M. Mabuchi : Effect of stress triaxiality on ductile fracture initiation low strength steels, *Journal of The Society of Materials Science of Japan*, Vol. 29, No. 322 (1976), pp. 717-723
8. H. Shimanuki, H. Furuya, T. Inoue, Y. Hagiwara and M. Toyoda : Effect of stress triaxiality and strain rate on ductile fracture initiation in steel, *Journal of The Society of Naval Architects of Japan*, Vol. 186, (1999), pp. 475-483
9. M. Toyoda, M. Ohata, N. Ayukawa, G. Ohwaki, Y. Ueda and I. Takeuchi : Ductile fracture initiation behavior of pipe under a large scale of cyclic bending, *Proc. 3rd Int. Pipeline Technology Conf.*, Brugge, Belgium , Vol. 2, (2000), pp. 87-102
10. O. Yasuda, M. Hirono, M. Yokota, M. Ohata and M. Toyoda : Criterion for ductile crack initiation of structure steel under a large scale of cyclic loading, *Journal of Constructional Steel*, Vol. 8, (2000), pp. 425-432
11. H. K. Sorensen : ABAQUS/Standard user's manuals, Ver. 5.8, (1998), 1 to 3
12. U. S .Lindholm, A. Nagy, G. R. Johnson and J. M. Hoegfeldt : Large strain, high strain rate testing of copper, *Transactions of the ASME. Journal of Engineering Materials and Technology*, Vol. 102, No. 4 (1983), pp. 376-381
13. M. R. Staker : The relation between adiabatic shear instability strain and material properties, *Acta Metallurgica*, Vol. 29, No. 4 (1981), pp. 683-689
14. S. L. Semiatin, M. R. Staker and J. J. Jonas : Plastic instability and flow localization in shear at high rates of deformation, *Acta Metallurgica*, Vol. 32, No. 9 (1984), pp. 1347-1354